Long-range and short-range magnetic order in β-HoH(D)$_{2+x}$ ($x=0$ and 0.12)

P. Vajda
Laboratoire des Solides Irradiés, CNRS-CEA, Ecole Polytechnique, F-91128 Palaiseau, France

G. André
Laboratoire Léon-Brillouin, CNRS-CEA Saclay, F-91191 Gif-sur-Yvette, France

O. J. Zogal
Institute of Low-Temperature and Structure Research PAN, PL 50-950 Wroclaw, Poland

(Received 27 October 1997)

The magnetic ordering existing at low temperatures in the stoichiometric dideuteride HoD_2 was investigated by powder neutron diffraction. Below the Néel temperature $T_2=6.3$ K, the magnetic structure is a modulated incommensurate antiferromagnet (AF), with a slightly temperature-dependent propagation vector. From $T_1 \sim 3$ to 4 K on and down to 1.4 K, it is coexisting with a commensurate AF configuration, modulated with a propagation vector $\mathbf{k}_1=\frac{1}{4}$ (113). The transition at T_1 is strongly hysteretic for both configurations, which is also manifest in electrical resistivity measurements. Magnetic fluctuations [short-range order (SRO) magnetism] are observed for $T>T_2$ up to nearly 45 K. The superstoichiometric compound $HoD_{2.12}$ exhibits quite intense SRO magnetism below $T=8$ K, which seems to be related to that existing for $T>T_2$ in the pure dideuteride HoD_2 and can be fitted in the hexagonal γ-phase cell. Attempts to observe ordering of the excess D atoms in the octahedral sublattice of $HoD_{2.12}$ below room temperature were unsuccessful despite strong indications towards such a phenomenon from resistivity and x-ray lattice-parameter measurements. [S0163-1829(98)05510-6]

I. INTRODUCTION

It was recognized some time ago[1] that the periodic moment structures in the antiferromagnetic (AF) state of the cubic rare-earth (R) dihydrides, whose modulation wave vectors were found to propagate in low-symmetry directions of the lattice, needed a special type of Fermi-surface nesting for their explanation. Thus, Liu[1] proposed for the propagation vector a form $\mathbf{k}=(\zeta,\zeta,1-\zeta)$, with ζ values of 0.5 and 0.75, which fitted quite satisfactorily the experimental situation at that time. On the other hand, it is also known[2] that the magnetic structures of many rare-earth based intermetallic systems are the result of the competition between long-range Ruderman-Kittel-Kasuya-Yosida (RKKY) exchange interactions and the interionic interactions, which often lead to frustrated situations producing modulated configurations with incommensurate wave vectors. It appears that a very similar situation exists in R-H systems where rather complicated magnetic phase diagrams are observed at low temperatures (for a comprehensive review, see, e.g., Ref. 3). Thus it was noted[4] that the heavy rare-earth dihydrides, β-RH_2 with R=Tb, Dy, Ho, and Er, exhibited commensurate AF configurations modulated along [113], whose magnetic moments were found to be parallel to [001] for R=Tb and Dy but close to [100] in the case of HoD_2; they were preceded by an ''intermediate'' structure before turning paramagnetic. This intermediate structure was determined in recent neutron-diffraction experiments for the cases β-TbD_2 (Ref. 5) and β-DyD_2 (Ref. 6) to be incommensurate, with a propagation vector $\mathbf{k}_i$ varying with temperature. Thus, for the former system, one had $\mathbf{k}_i(TbD_2)=\mathbf{k}_2\approx\frac{1}{8}$ (116) between T_2 $(=T_N)$ $=19$ and 14.8 K, while the low-T phase (overlapping in part the incommensurate one) was commensurate below T_1 $=16$ K, modulated with a propagation vector $\mathbf{k}_c(TbD_2)$ $=\mathbf{k}_1=\frac{1}{4}$ (113). For the second system, on the other hand, both the intermediate and the low-temperature (LT) phases were incommensurate: $\mathbf{k}_2(DyD_2)=(0.275, 0.275, 0.750)$, between 5 and 3 K, and $\mathbf{k}_1(DyD_2)=(0.258, 0.273, 0.750)$ below 3.5 K, both wave vectors being close to $\frac{1}{4}$ (113).

Another specific phenomenon, particular to the R hydrides, is the often dramatic influence of the octahedral (H_o) hydrogen atoms x, present interstitially in the fluorite-type lattice of superstoichiometric compounds β-$RH(D)_{2+x}$, upon their electronic and magnetic properties.[3] Thus, new commensurate and incommensurate structures were introduced in β-TbD_{2+x} for x between 0.15 and the phase limit $x^{\beta}_{\max}(Tb)\sim 0.25$ (Ref. 5), while only traces of short-range-ordered (SRO) magnetism were detected in β-DyD_{2+x}, with $x=0.135$ (Ref. 6). Another exciting property, closely related to the formation of an ordered H_o sublattice above a certain x concentration and below a certain temperature, is the manifestation of metal-semiconductor transitions as observed by electrical resistivity measurements for several RH_{2+x} systems.[3] The ordered H_o sublattice had been identified[7] in β-TbD_{2+x} as a Ni_3Mo-type structure of tetragonal symmetry, DO_{22}.

The earliest reliable observations of magnetic transitions in HoH_2 were done by specific-heat measurements[8] and Mössbauer effect,[9] giving a T_N of 5.2 to 5.4 K. Related low-T specific-heat,[10] neutron-inelastic-scattering,[11] and resistivity[12] experiments were mainly used to study the crystalline electric fields in $HoH(D)_2$. After a first unsuccessful attempt to characterize the observed neutron-diffraction spectrum by Cox *et al.*,[13] Shaked *et al.*[4] had determined the magnetic structure of the commensurate LT phase in HoD_2

and established the existence of an intermediate phase. Finally, detailed LT-susceptibility[14] and electrical resistivity[15] measurements through the whole existence range of the β phase disclosed the fine structure of the magnetic transitions in the pure dihydride, $x=0$. As to the superstoichiometric dihydrides, only the Mössbauer study on Er:$HoH_{2.04}$ by Friedt *et al.*[9] furnished a qualitative indication for the presence of a noncubic crystal field, before the complete susceptibility[14] and resistivity[15] investigations mentioned above showed the evolution from magnetic long-range order (LRO) to SRO with growing x. A tentative magnetic phase diagram had issued from the latter studies.

It seemed important to analyze the magnetic structure in the system β-$HoH(D)_{2+x}$ and to compare with the earlier investigated β-$TbH(D)_{2+x}$ (Ref. 5) and β-$DyH(D)_{2+x}$,[6] in view of the similarities and the differences between the two latter. For this purpose, we have undertaken a neutron-diffraction investigation through the whole magnetically ordered temperature range and determined the prevailing magnetic configurations in the pure dideuteride β-HoD_2, refining the data reported by Shaked *et al.*[4] and disclosing new phenomena, such as the coexistence of commensurate and incommensurate phases down to the lowest temperatures and the presence of SRO magnetism quite above T_N. For the superstoichiometric compound β-HoD_{2+x}, we have selected a concentration $x=0.12$, a value hopefully large enough to permit the neutron-diffraction observation of H_o-sublattice ordering following the indications from resistivity and x-ray lattice-parameter measurements. At the same time, we are going to analyze the well-developed magnetic SRO present in $x=0.12$ below $T\sim 8$ K and that seems to be related to the SRO observed for $x=0$ above T_N.

II. EXPERIMENTAL

The samples for the diffraction studies were prepared from nominally 4N holmium ingots purchased from the Ames Laboratory (Ames, Iowa), containing (in at. ppm) as main metallic impurities: 45 Fe, 30 Ta, 6 Hf, 5 Cr, 5 Ni, 3 Cu, 3 Zr, and 10 ppm other rare earths; and as major gaseous solutes: 650 at. ppm H, 600 F, 310 O, and 300 C. 1 to 2 g ingots were loaded with deuterium according to the two-step procedure described in detail in Ref. 3: (i) the preparation of the ''pure'' dideuteride by filling all available tetrahedral sites at 550–600 °C followed by pumping off any D atoms on octahedral sites; (ii) adding the octahedral x atoms at 300–350 °C to yield the superstoichiometric compound. The final specimens of the compositions $HoD_{2.005(5)}$ and $HoD_{2.12(1)}$ were crushed to powder and used for both the neutron- and the x-ray-diffraction investigations. The resistivity samples were hydrogen-loaded $18\times1\times0.2$ mm^3 foils, provided with four platinum contacts, analogous to those described in Ref. 15. The data presented here are actually in part unpublished results from that study and further experimental details can be found there. The used concentrations $x=0$ and $x=0.12$ are based on a ''pure'' dihydride of the composition $HoH_{1.99(1)}$.

The neutron-diffraction spectra were taken on the G4.1 spectrometer situated at the cold-neutron guide of the Orphée reactor of the Laboratoire Léon-Brillouin at Saclay, employing an 800 cell multidetector in the range $12°\leqslant 2\Theta\leqslant 92°$ and a neutron wavelength $\lambda=2.425$ Å, in the temperature interval $1.4\leqslant T\leqslant 45$ K. Additional spectra were taken at room temperature and at 240 K when searching for H_o-sublattice ordering. For the same purpose, we had applied various cooling rates across the critical range between 100 and 250 K: from ~ 0.1 to several 10^2 K/min. The data analysis was performed using the Rietveld-type program FULLPROF.[16]

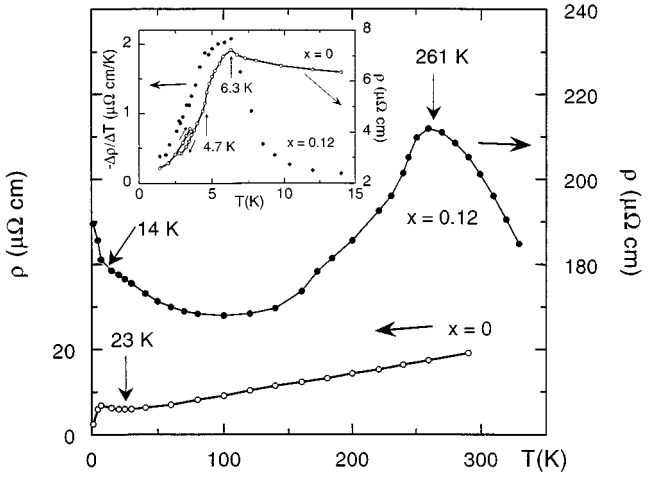

FIG. 1. Temperature dependence of the electrical resistivity of β-HoH_{2+x}, with $x=0$ (open signs) and $x=0.12$ (full signs). Inset: enlarged view of the low-T resistivity for the $x=0$ sample and of the derivative, $-\Delta\rho/\Delta T$, for the $x=0.12$ sample, in the magnetically ordered region. The indicated temperatures correspond to special points as discussed in the text.

The lattice parameters a of both samples were determined by x-ray diffractometry, employing Cu Kα radiation, and using a Siemens D-5000 powder diffractometer equipped with an A.Paar He-TTK low-temperature attachment working under dynamic vacuum. The measuring precision on a single $a(T)$ point was better than $\pm 1\times10^{-3}$ Å.

III. RESULTS AND DISCUSSION

In what follows, we shall first present the results of the investigations pertaining to hydrogen ordering, i.e., those performed in the interval up to room temperature, while the second part will concern in more detail the low-T region of magnetic ordering.

A. Hydrogen ordering

1. Electrical resistivity

Figure 1 shows the resistivity of both hydrogen compositions through the whole measured temperature range. The pure dihydride $x=0$ has been partly taken over from Ref. 15 and serves as a base to compare with. There is not much to be emphasized here besides the low-T magnetically ordered part whose fine structure is shown in more detail in the inset and shall be treated later.

The $x=0.12$ sample, on the other hand, exhibits all the interesting features such as discussed in Ref. 15 for the x-rich specimens. We note, with increasing temperature, a semiconducting region due to carrier localization caused by

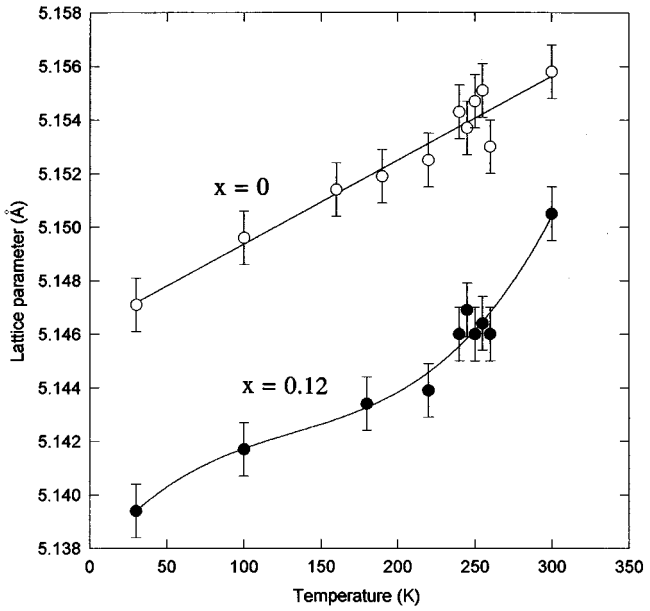

FIG. 2. X-ray lattice parameters of β-HoD_{2+x}, with $x=0$ and $x=0.12$, as a function of temperature. The s shape in the latter case is an indication for D_o-sublattice ordering below ~ 250 K.

atomic disorder and ending near 100 K, followed by a metallic part due to the formation of a delocalized band near the Fermi level driven by the ordering of the octahedral x atoms in this T range, and finishing by a metal-semiconductor transition at $T_{MS}=261$ K when the delocalized band breaks up. Again, as for the $x=0$ sample, there is some structure due to magnetic manifestations superimposed below ~ 7 K, which is shown in the inset in differentiated form and will be discussed later together with the neutron data.

2. X-ray lattice parameters

The temperature dependence of the lattice parameters for the two specimens used in the neutron experiments were measured by x-ray diffraction and are shown in Fig. 2. The qualitative change when going from the pure dideuteride to the superstoichiometric is, first, the lattice contraction due to the increasingly ionic attractive interaction with the introduced octahedral D atoms and well known from other β-$RH(D)_{2+x}$ systems;[3] second, the nonlinear behavior, whose s shape is a strong indication of superlattice formation and has been observed recently in β-RH_{2+x} compounds with R=Y, Gd, Tb, and Dy, for high x values.[17]

The room-temperature lattice constant for the $x=0$ sample, $a(HoD_2)=5.155(1)$ Å, compares favorably with the only published value by Pebler and Wallace,[18] for the hydride, $a(HoH_2)=5.165$ Å, the difference of 10×10^{-3} Å corresponding to the isotope effect in other RH_2 systems.[3] The linear slope in Fig. 2 for this specimen gives a thermal expansion coefficient between 30 and 300 K of

$$\alpha=(1/a)\Delta a/\Delta T=6.0(5)\times10^{-6}/\mathrm{K}\ \text{ for }\ HoD_2,$$

which is very close to the α values from Ref. 17; the contraction observed between the two D concentrations would correspond, in a linear interpolation, to a coefficient $\beta=(1/a)\Delta a/\Delta x$, at the respective temperatures

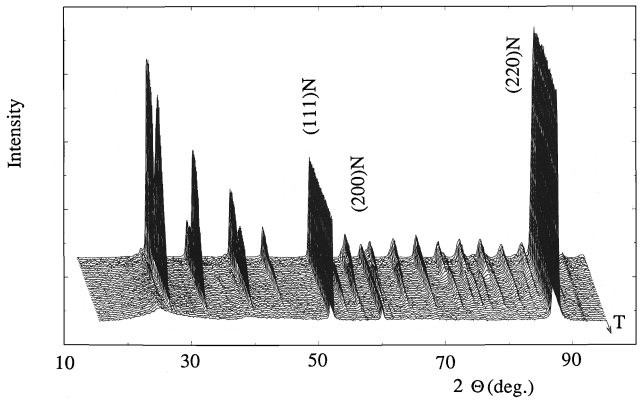

FIG. 3. Neutron-diffraction spectra of HoD_2 in the range $1.4\leqslant T\leqslant 7$ K, showing the fine structure and the evolution of the magnetic peaks.

$$\beta_{30\ \mathrm{K}}=-1.25(10)\times10^{-2}/\text{atom D}$$

and

$$\beta_{300\ \mathrm{K}}=-0.85(10)\times10^{-2}/\text{atom D},$$

i.e., some 30% stronger in the low-T ordered state.

3. Neutron diffraction

Having observed strong indications towards x-sublattice ordering in the region around 250 K in the $x=0.12$ specimens both from the $\rho(T)$ and the $a(T)$ dependences (Figs. 1 and 2) and in view of the successful experiment on β-TbD_{2+x} (Ref. 7) for $0.10\leqslant x\leqslant 0.25$, we have investigated several neutron-diffraction spectra of $HoD_{2.12}$ in the critical range very thoroughly, in the search of any superstructure lines. Unfortunately, despite a rather high signal-to-background ratio and a good instrumental resolution, we could not detect any structure attributable to a D_o superlattice. The only additional lines were traces of a few percent hexagonal γ-HoD_3 precipitates, which is a proof that the sample was very close to the β-phase limit, with small parts overlapping into the two-phase region. Thus, although practically at the phase boundary, the x concentration in $HoD_{2.12}$ seems not sufficient to make the ordering transition visible by neutron diffraction. Another possibility is an insufficiently developed LRO of the D_o superlattice leading to broadening and practical disappearance of the superstructure lines, although the ordering seems strong enough in the macroscopic measurements described above. A spectroscopic confirmation of the DO_{22} structure as seen in β-TbD_{2+x} (Ref. 7) remains, therefore, open and highly desirable for other RD_{2+x} systems.

B. Magnetism

1. x=0

As can be seen in the inset of Fig. 1, the resistivity of HoH_2 exhibits two additional transition regions below the Néel temperature $T_N=T_2=6.3$ K: a change in slope at 4.7 K and a hysteretic break between 2.5 and 3.5 K, in agreement with the susceptibility data of Boukraa and co-workers.[14] Shaked *et al.*[4] had reported only one additional transition, at 4.5 K, for the disappearance of the ''intermedi-

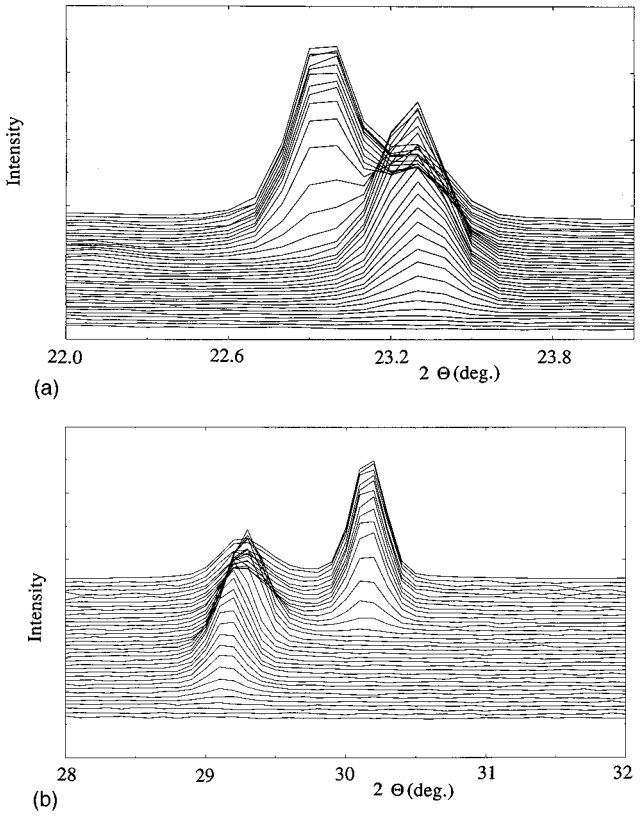

FIG. 4. Evolution with temperature of the principal magnetic lines of the spectra in Fig. 3, showing the varying behavior of their sublines. (a) at $2\Theta \sim 23°$; (b) at $2\Theta \sim 30°$.

ate'' phase and the (simultaneous) growth of the LT commensurate phase. We took, therefore, particular care by measuring 36 complete spectra in the interval 1.4 through 7 K and discovered, actually, more details than expected even after the resistivity results.

Figure 3 presents a three-dimensional plot of the neutron spectra up to $T=7$ K, showing qualitative similarity with the spectra of Ref. 4 but disclosing many surprising details. One notes, in fact, the simultaneous presence of two magnetic configurations down to the lowest temperatures, which follow different thermal evolutions. This behavior is illustrated, for example, through the isothermals of the first two line systems in Fig. 3, around $2\Theta=23°$ [Fig. 4(a)] and $2\Theta=30°$ [Fig. 4(b)], denoted respectively (113) and (331) in Ref. 4. One can observe the apparently correlated decrease and increase with T of the subline amplitudes at $2\Theta=23.0°$ and 23.3° [Fig. 4(a)], but also the varying position of the subline at $2\Theta=29.3°$ shifting gradually towards 29.1° between 3.8 and 6.4 K [Fig. 4(b)] indicating a temperature variation of the magnetic propagation vector. No splitting of the (113) or (331) lines had been resolved in Ref. 4.

Figure 5 summarizes the thermal comportment of the two configurations as measured on the (331) line group with increasing and with decreasing temperature. We note strong hysteretic behavior for both configurations in the region between 2 and 4 K, the width of the hysteresis being somewhat narrower, $\Delta T \sim 1$ K, in the case of the LT configuration. This is a beautiful confirmation of the hysteretic domain in resistivity as shown in the inset of Fig. 1 (where it represents in

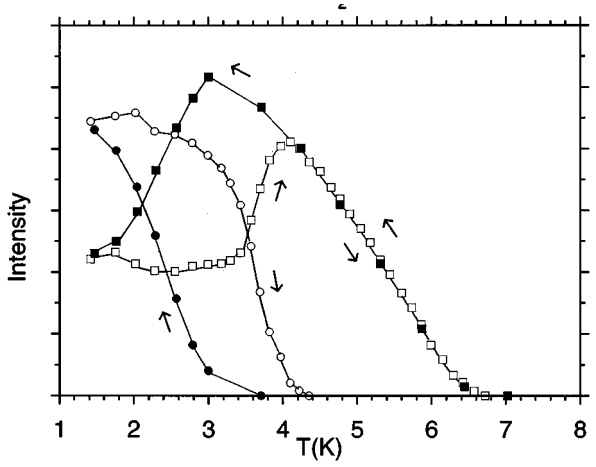

FIG. 5. Temperature dependence of the integrated intensities, taken on the group of $(111)^-$ lines at $2\Theta \sim 30°$ [Fig. 4(b)], of the commensurate (circles) and the incommensurate (squares) configurations. Note the strongly hysteretic behavior in the region of T_1, at ~ 2.0 to 3.5 K.

an enhanced manner the manifestations of both magnetic configurations). At the same time, it might explain the surprising time dependence of some magnetic lines described by Cox *et al.*[13] in HoD_2 around 4 K by their inherent instability in this range.

The second unusual observation is the presence of the ''intermediate'' configuration down to the lowest temperatures together with the LT structure. This had not been the case for TbD_2 (Ref. 5) neither for DyD_2,[6] where there existed an overlap interval for the two magnetic phases of a relative width $\delta T/T_1 \sim 0.1$ and where the intermediate phase vanished, in principle, for $T<T_1$. Thus, in the case of HoD_2, it seems no longer justified to call the higher-T phase ''intermediate.''

We have determined the magnetic structure of the prevailing configurations and are showing the diffraction spectra and some of the corresponding best fits at three typical temperatures below T_1, between T_1 and T_2, and just below T_2, in Fig. 6: (i) Fig. 6(a), at 1.4 K, exhibits both the commensurate and the incommensurate phases present; (ii) Fig. 6(b), at 4.5 K, has only the incommensurate phase left, but a short-range magnetism begins to appear as broadening at the base of the main magnetic lines; (iii) Fig. 6(c), finally, taken at 6.42 K, presents well-developed magnetic SRO lines, with the rest of the incommensurate phase.

The commensurate phase observed below the hysteresis domain around T_1 corresponds to modulated antiferromagnetism with a propagation vector $\mathbf{k}_1=\frac{1}{4}$ (113), in agreement with the measurements by Shaked *et al.*,[4] and also with the low-T configuration in β-TbD_2 (Refs. 4 and 5) but not in β-DyD_2 (Ref. 6) that was found to be incommensurate. For this commensurate phase, the magnetic-moment amplitude on the Ho atoms is independent of their positions and the refinement gives, at 1.4 K, $|M_c|=5.76(3)\ \mu_B$, with a common moment direction characterized by the components $\mathbf{M}_c(\mu_B)=(4.63,-2.67,-2.14)$. This amplitude $|M_c|$ is smaller than Shaked's 6.4(4) μ_B as it does not contain the magnetic moment of the incommensurate phase coexisting in this temperature range. The latter is characterized by a propa-

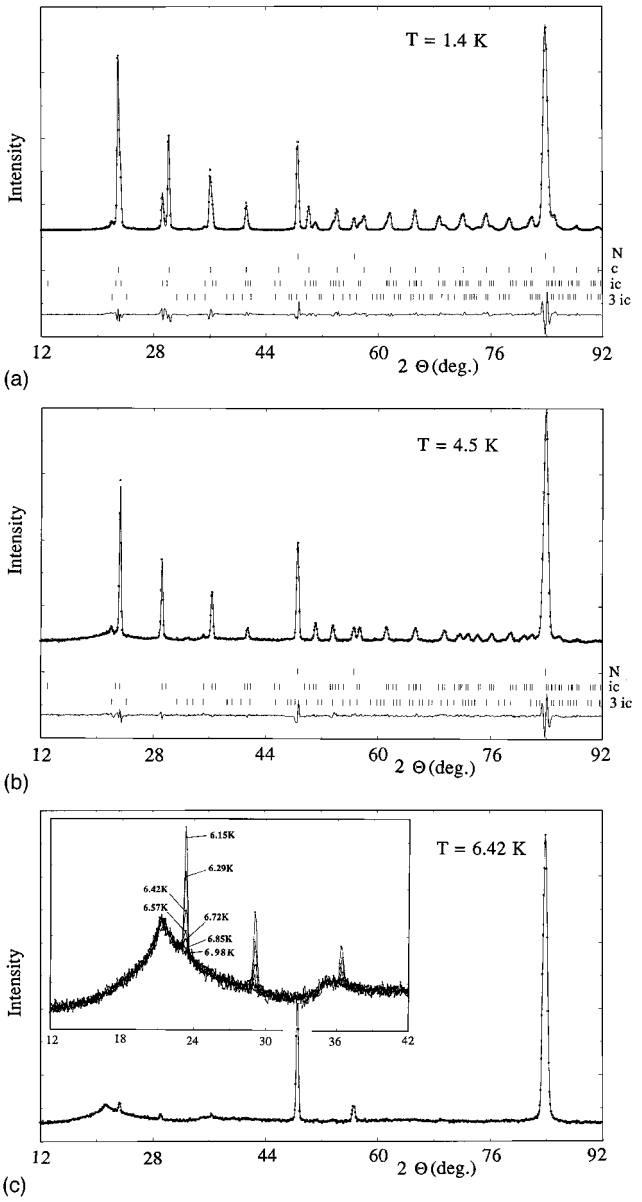

FIG. 6. Neutron spectra of HoD_2 at three typical temperatures and their best fits for the two lower ones. (a) $T=1.4$ K; (b) $T=4.5$ K; and (c) $T=6.42$ K. The vertical marks indicate the positions of the various corresponding configurations employed, with the respective $\mathbf{k}_1$, $\mathbf{k}_2$, and $3\mathbf{k}_2$; the SRO-M fit for Fig. 6(c) corresponds to that for $HoD_{2.12}$ and is shown in Fig. 8. Inset in Fig. 6(c): enlarged view in the interval $6.15 \leqslant T \leqslant 7$ K, showing the asymmetry of the two main SRO lines.

gation vector $\mathbf{k}_2(1.4\text{ K})=[0.2731(1), 0.2731(1), 0.7482(2)]$, close to but yet significantly different from $\mathbf{k}_1$. Moreover, as is visible in Fig. 6(a), small extra magnetic peaks are still observed and can be nicely indexed as corresponding to $3\mathbf{k}_2$. The refinement given in Fig. 6(a) for this incommensurate phase yields a moment-amplitude ratio $|M_{3k2}|/|M_{k2}| \approx \frac{1}{3}$, thus perfectly corresponding to a square modulation. This leads to a constant moment on the Ho atoms giving $|M_{ic}|=4.03(4)\ \mu_B$ with a moment direction $\mathbf{M}_{ic}(\mu_B)=(3.64, -1.64, 0.54)$. The resulting maximum total moment at low temperatures is $|M_1|=7.0(1)\ \mu_B$, somewhat bigger than the value determined in Ref. 4 but still significantly less than the 10 μ_B of the free Ho^{3+} ion. These authors had attributed the low magnetic moment to a quenching by the crystal field and a possible loss to conduction electrons. We believe, however, that the clearly present magnetic SRO within the long-range-ordered interval [Fig. 6(c) but also Fig. 6(b)], though difficult to estimate, should make a non-negligible contribution to the total moment. The reliability factors for the nuclear Bragg reflections and for the two magnetic contributions are, respectively, $R_N=1.4\%$, $R_{Mc}=4.2\%$, $R_{Mic}=6.2\%$.

In the temperature range $T_1 \leqslant T \leqslant T_2$ [Fig. 6(b)], the commensurate phase has vanished, and one obtains the best fit, at 4.5 K (with increasing T), using a propagation vector $\mathbf{k}_2(4.5\text{ K})=[0.2740(1), 0.2740(1), 0.7474(1)]$, indicating a very small but, in view of the high reliability, non-negligible temperature-dependent drift away from the commensurability value (0.25, 0.25, 0.75). The modulation is still squared, with an amplitude $|M_{ic}|=5.38(3)\ \mu_B$ and with a moment direction $\mathbf{M}_{ic}(\mu_B)=(4.68, -2.58, 0.63)$. The reliability factors are $R_N=1.5\%$ and $R_{Mic}=3.0\%$.

The magnetic moment associated with this incommensurate phase has thus grown from that at the lowest temperature, as is reflected through the variation of the magnetic peak intensity in Fig. 5. As the temperature increases from T_1, the incommensurate modulation remains squared up to $T \approx 4.9$ K where the $3\mathbf{k}_2$ harmonics contribution begins to decrease progressively and finally disappears near 5.5 K. Hence, from 5.5 K to T_2, the incommensurate modulation turns purely sinusoidal. As concerns the behavior of the propagation vector $\mathbf{k}_2$ between T_1 and T_2, it continues to vary slightly away from $\mathbf{k}_1$ to reach the value $\mathbf{k}_2=[0.2765(2), 0.2765(2), 0.7464(4)]$ at 6 K. The same remarks concerning the contribution of magnetic SRO as in the previous paragraph are also valid here.

The spectrum in Fig. 6(c), taken at $T=6.4$ K and where the rest of the incommensurate lines can be seen, is notable for its clearly developed SRO peaks centered at $2\Theta \sim 21°$ and at $2\Theta \sim 35°$. These peaks had already begun to show up at 4.5 K [Fig. 6(b)] as broadening near the main magnetic *ic* lines and persist to rather high temperatures, up to ~ 45 K. A fit of these peaks was not very satisfactory and we shall postpone its discussion to Sec. III B 2 where the superstoichiometric compound $HoD_{2.12}$ is shown to exhibit analogous but much stronger SRO lines *below* 7 K. But already now we wish to draw attention to the striking asymmetry of both SRO peaks, with the right-hand shoulder extending towards higher angles [inset in Fig. 6(c)]: a first indication of possible anisotropy.

Figure 7 permits to visualize the thermal evolution of the main SRO peak at $2\Theta=21.5°$ in the range from 7 K through 45 K, roughly at the limit of detectability. This is again quite compatible with the resistivity data of Fig. 1 where the ρ decrease above the Néel temperature of 6.3 K can be a manifestation of critical magnetic fluctuations. The temperature of the minimum itself, 23 K, is the result of a competition between decreasing SRO and increasing phonon contributions with T. It is interesting to note that neither TbD_2 (Ref. 5) and DyD_2,[6] in neutron diffraction and resistivity, nor ErH_2 (Ref. 19) and GdH_2,[20] in resistivity, did show any sign of SRO above the ordered AF range. One might wonder if the par-

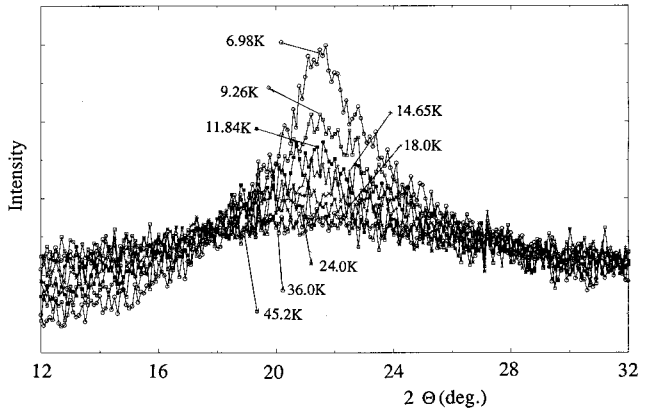

FIG. 7. Thermal evolution of the SRO peak at $2\Theta \sim 21.5°$ in HoD_2 in the interval $6.4 \leqslant T \leqslant 45$ K. Note the rest of the sublines at $2\Theta = 23.2°$ and $2\Theta = 29.1°$ belonging to the configuration with $\mathbf{k}_2$ below 7 K.

ticular strength of the incommensurate phase in HoD_2, which persists below T_1 down to the lowest temperatures, is related to the same phenomenon which is also responsible for the far reaching magnetic fluctuations above T_2. As to the size of the magnetic SRO domains, they reach from $\lambda_{SRO} = 55$ Å at 7 K to $\lambda_{SRO} = 30$ Å at 45 K.

2. x = 0.12

The neutron spectrum of $HoD_{2.12}$ taken at 1.4 K (Fig. 8) exhibits broad but rather intense peaks of magnetic origin indicative of SRO. It is remarkable that their positions (at least those of the clearly identifiable lines at $2\Theta \sim 21.5°$ and $2\Theta \sim 34.5°$) are practically coinciding with the SRO peaks of the $x = 0$ specimen above $T \sim 6$ K, even when allowing for the lattice contraction in $HoD_{2.12}$ (cf. Fig. 2).

As already mentioned in the preceding subsection, a fit of the SRO lines was not easy to achieve, especially when trying to use the fcc β-phase cell as base unit. Neither had we succeeded in applying a tetragonal distortion, which might have resulted from a possible ordering of the octahedral excess deuterium atoms (see e.g., Refs. 3 or 7). On the other hand, a reasonable fit could be obtained when using the hexagonal structure of the γ-phase trihydride, with the parameters $a = 3.547$ Å and $c = 6.639$ Å, as shown through the SRO-M ticks in Fig. 8 together with the perfect fcc β-phase fit of the nuclear lines. Note also the presence of traces of the γ phase at higher angles [in particular on the right-hand shoulder of the (220) line] corresponding to a few percent of HoD_3 and already mentioned in Sec. III A 3. Nothing is known about the magnetism of the trihydride but its responsibility for the SRO lines observed in the neutron spectrum of Fig. 8 can be excluded already for intensity reasons, in the same way as the possible presence of $Ho(OD)_3$, ferromagnetic below 2.5 K.[21]

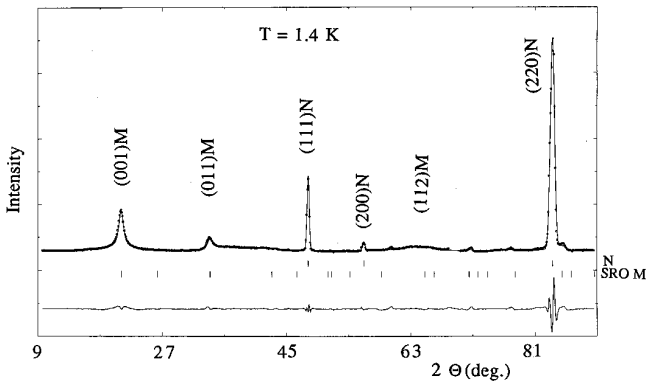

FIG. 8. Neutron spectra of $HoD_{2.12}$ at 1.4 K. The best fit of the magnetic SRO peaks is indicated through the corresponding vertical marks. Note also the presence, at higher angles, of a small peak corresponding to a few percent of γ-HoD_3 phase.

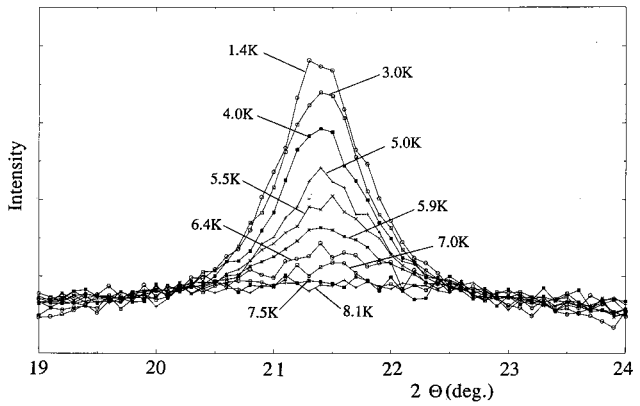

FIG. 9. Thermal evolution of the SRO peak at $2\Theta \sim 21.4°$ in $HoD_{2.12}$ in the interval $1.4 \leqslant T \leqslant 8$ K.

This fit using the hexagonal cell of the trihydride is *a priori* troubling, even if the resulting parameters are not exactly the measured ones for γ-HoD_3, $a = 3.64$ Å and $c = 6.56$ Å. On the other hand, it turns out that the fcc unit cell of the β phase and the hcp cell of the γ phase are related. In our particular case, with $a_{fcc}(HoD_2) = 5.15$ Å (cf. Fig. 2) and $a_{hcp}(HoD_3) = 3.64$ Å, we have immediately $a_{fcc}/\sqrt{2} = a_{hcp}$, strongly suggesting a relation $[110] \| [11\text{–}20]$ and $(111) \| (0001)$, such as observed for martensitic transformations fcc↔hcp in certain metals and alloys (see e.g., Ref. 22). (In reality, the crystal structure of the γ phase is more complicated,[23] D^4_{3d}, but this lower symmetry concerns only the deuterium sites and is of no consequence for our discussion.)

As to the asymmetric shape of the peaks, apparently more developed in the case of the (011) SRO-M peak near 35° [see also inset of Fig. 6(c)], it could indicate a quasi-two-dimensional order, with more ordering along the c axis.

The magnetic SRO structure disappears above ~ 8 K, as can be seen in Fig. 9 following the isothermals of the main line at $2\Theta = 21.5°$. The analysis of the linewidths yields a domain-size variation from $\lambda_{SRO} \sim 300$ Å to ~ 50 Å when going from 1.4 to 8 K, with practically the same value at a temperature of 7 K as for the SRO peak in Fig. 7 in the case of the $x = 0$ specimen. Note also that the break in the slope of the resistivity at 6.3 K in the inset of Fig. 1 for the $x = 0.12$ sample corresponds rather closely to the vanishing temperature of the SRO peaks. Similarly, the flat peaks in susceptibility[14] in HoH_{2+x}, $x > 0.06$, and the broadening of the Mössbauer spectrum[9] in $HoH_{2.04}$ (with an undetermined x value), suggesting magnetic SRO, find here direct confirmation by neutron scattering. The slope minimum in resis-

tivity near 14 K (Fig. 1), observed in all β-HoH_{2+x} specimens with $x>0.1$ and tentatively attributed in Ref. 15 to the limit of the SRO phase, should now be viewed rather as a kind of ''compromise'' temperature between the downturn towards the residual resistivity and the upturn driven by magnetic fluctuations. The upper limit of the SRO region in the phase diagram should now be set at ~ 8 K.

IV. CONCLUSIONS

High-sensitivity cold-neutron-diffraction experiments have been used to investigate eventual sublattice ordering of the octahedral hydrogen atoms in the superstoichiometric compound $HoH(D)_{2.12}$. Despite strong indications towards such an ordering from electrical resistivity as well as from x-ray lattice-parameter measurements as a function of temperature, the x concentration is apparently too low or the LRO of the superstructure not enough developed to permit the detection of the ordered superlattice by neutrons.

On the other hand, we have succeeded to determine and to characterize all existing magnetic configurations in the pure ($x=0$) dideuteride, HoD_2: (i) an incommensurate modulated structure, below $T_2=6.3$ K, with a (slightly temperature-dependent) propagation vector $\mathbf{k}_2(1.4\text{ K}) \approx (0.273, 0.273, 0.748)$; (ii) joined, from $T_1 \approx 3$ to 4 K on, by a commensurate AF configuration with a propagation vector $\mathbf{k}_1=\frac{1}{4}$ (113), the two structures coexist down to the lowest temperatures measured, 1.4 K; the transition at T_1 is strongly hysteretic for both configurations; (iii) anisotropic SRO magnetism is observed above T_2 and remains detectible up to nearly 45 K.

The neutron spectrum of the superstoichiometric compound $HoD_{2.12}$ exhibits, below 7 K, rather intense SRO magnetic peaks, apparently related to the SRO magnetism observed in pure HoD_2 above T_2.

Thus, when analyzing the magnetic structures of the three β-$RH(D)_2$ systems with R=Tb,[5] Dy,[6] and Ho (this work), one notes that the suggestion by Liu[1] as to a sinusoidally modulated AF configuration with $\mathbf{k}=(\zeta,\zeta,1\text{-}\zeta)$ is qualitatively confirmed, with $\zeta=\frac{1}{4}$, for the low-T structures propagating with $\mathbf{k}_1$. On the other hand, the observation of an intermediate AF structure with an incommensurate propagation vector $\mathbf{k}_2$, before the paramagnetic region, is not predicted by the nesting features of the Fermi surface but rather follows from the frustrated situation between the RKKY interactions and the crystal field. In the cases of R=Dy and Ho, $\mathbf{k}_2$ is close to $(\zeta,\zeta,1\text{-}\zeta)$ while, for R=Tb, it is rather $\sim(\zeta,\zeta,1\text{-}2\zeta)$. For the superstoichiometric systems, the situation appears to be quite complicated and varying from one compound to another: in TbD_{2+x}, one has $\mathbf{k}_1 \sim (\zeta,\zeta,1)$ and $\mathbf{k}_2 \sim (\zeta_1,\zeta_2,1)$ for $x=0.18$ and 0.24; in DyD_{2+x} with $x=0.135$, we only observe weak SRO; and in HoD_{2+x} with $x=0.12$, the strong SRO present at low T resembles much the far-reaching SRO of the pure HoD_2 above T_N.

It will be interesting to investigate the system β-ErD_{2+x}, both as concerns the analysis of the prevailing magnetic configurations and the coexistence range of the structures with $\mathbf{k}_1$ and $\mathbf{k}_2$ as well as the possible observation of magnetic SRO. Work in this direction is in progress.

ACKNOWLEDGMENT

We are grateful to Dr. J. Janczak (Wroclaw) who performed the x-ray-diffraction measurements.

[1] S. H. Liu, Solid State Commun. **61**, 89 (1987).
[2] D. Gignoux and D. Schmitt, Phys. Rev. B **48**, 12 682 (1993).
[3] P. Vajda, in *Handbook on the Physics and Chemistry of Rare Earths*, edited by K. A. Gschneidner (North-Holland, Amsterdam, 1995), Vol. 20, p. 207.
[4] H. Shaked, D. G. Westlake, J. Faber, and M. H. Mueller, Phys. Rev. B **30**, 328 (1984).
[5] P. Vajda, J. N. Daou, and G. André, Phys. Rev. B **48**, 6116 (1993).
[6] P. Vajda, G. André, and J. Hammann, Phys. Rev. B **55**, 3028 (1997).
[7] G. André, O. Blaschko, W. Schwarz, J. N. Daou, and P. Vajda, Phys. Rev. B **46**, 8644 (1992).
[8] Z. Bieganski and B. Stalinski, J. Less-Common Met. **49**, 421 (1976).
[9] J. M. Friedt, B. Suits, G. K. Shenoy, B. D. Dunlap, and D. G. Westlake, J. Appl. Phys. **50**, 2049 (1979).
[10] Z. Bieganski, J. Opyrchal, M. Drulis, Bull. Acad. Pol. Sci. Ser. Sci. Chim. **XXI**, 703 (1973).
[11] N. Shamir and H. Shaked, Phys. Rev. B **22**, 6463 (1980).
[12] J. N. Daou, P. Vajda, and J. P. Burger, Phys. Rev. B **37**, 5236 (1988).
[13] D. E. Cox, G. Shirane, W. J. Takei, and W. E. Wallace, J. Appl. Phys. **34**, 1352 (1963).
[14] A. Boukraa, P. Vajda, and J. N. Daou, Z. Phys. Chem. (Munich) **179**, 413 (1993).
[15] J. N. Daou and P. Vajda, Phys. Rev. B **50**, 12 635 (1994).
[16] J. Rodriguez-Carvajal, Physica B **192**, 55 (1993).
[17] M. Chiheb, J. N. Daou, and P. Vajda, Z. Phys. Chem. (Munich) **179**, 255 (1993).
[18] A. Pebler and W. E. Wallace, J. Phys. Chem. **66**, 148 (1962).
[19] P. Vajda and J. N. Daou, Phys. Rev. B **49**, 3275 (1994).
[20] P. Vajda, J. N. Daou, and J. P. Burger, J. Less-Common Met. **172/174**, 271 (1991).
[21] C. A. Catanese and H. E. Meissner, Phys. Rev. B **8**, 2060 (1973).
[22] J. W. Christian, *Theory of Transformations in Metals and Alloys* (Pergamon, New York, 1965).
[23] W. Mansmann and W. E. Wallace, J. Phys. (Paris) **25**, 454 (1964).